Continuous spectra of protons and deuterons from the $\alpha + \alpha$ interaction in the incident energy interval 110–172 MeV

G. Paić and B. Antolković
Institut "Rudjer Bošković," Zagreb, Yugoslavia

A. Djaloeis, J. Bojowald, and C. Mayer Böricke
Institut für Kernphysik, KFA, Jülich, West Germany

(Received 3 October 1980)

The inclusive proton and deuteron spectra from the $\alpha + \alpha$ interaction at $E_\alpha = 110$, 130, 158, and 172 MeV measured in the angular range $9° \leq \theta_{lab} \leq 50°$ are presented. The shape of the spectra are satisfactorily fitted using the Fermi statistical partition model which yields spectra whose shape are dictated by the phase space allowed to the particles present in the final state. The success of this model points to the importance of that mode of breakup in nuclear reactions below the pion production threshold.

[NUCLEAR REACTIONS ^{4}He(α,x); $x = p, d$, $E = 110-172$ MeV; measured $\sigma(E,\theta)$; statistical partition-model analysis; deduced contribution strength of various breakup modes. Gas target.]

I. INTRODUCTION

Energy spectra of particles from nuclear reactions generally contain continuum parts. In reactions among light nuclei these continua can be attributed to the following processes: (i) transitions to broad resonance levels, (ii) peripheral phenomena, such as quasifree scattering or final-state interactions, (iii) rescattering in the volume of the interaction, and (iv) fusionlike phenomena resulting in several particles in the outgoing channel.

Usually several, if not all, of these processes are present. While the processes (i), (ii), and (iii) have been extensively studied,[1–3] the processes of type (iv) have not received much attention. However, it is a fact that at moderately high incident energies there is always a part of the spectrum which cannot be associated with processes (i)–(iii). This unexplained part of the spectrum is usually spread over the whole energy range available (excluding of course the region of the discrete bound states). On it, more readily identifiable structures (e.g., resonance levels) are sometimes superimposed. A better knowledge of the processes responsible for this continuous "background" is desirable for several reasons:

(a) The continuum generally constitutes an important, if not major, portion of the integrated spectrum.

(b) Correct subtraction of the continuum from the total spectrum is needed whenever information on the position and shape of the superimposed peaks is required.

(c) So far very little is known about the energy dependence and angular distribution of the continuum.

It is, therefore, of interest to focus attention specifically on that part of the spectrum and to compare the results with simple theoretical predictions.

The α-induced breakup of the alpha particle is a favorable case for such an investigation. The reason is that, in view of the high binding energy of the alpha particle, the probability for quasifree scattering is expected to be much lower than that in the case for a more loosely bound projectile or target.

The present experiment has as objectives to measure the shape of the continuous particle spectra of emitted protons and deuterons; measure the dependence of the shape of the spectra and of the corresponding "decay" modes on the energy available in the center of mass; and measure the dependence of

the shape at inclusive spectra on the angle of emission.

II. EXPERIMENT

The measurements were performed with the unanalyzed alpha particle beam of the variable energy cyclotron JULIC. The energy resolution and the relative uncertainty in the energy calibration were both about 0.3%. The beam spot was 2–3 mm in diameter in the center of the $\phi = 1$ m scattering chamber. The target ^{4}He gas was contained at $p = 450$ Torr and $T = 25$ °C in a $\phi = 60$ mm gas cell with 2.2 μm thick Havar windows. The p and T values were read periodically and found to be constant within 2% and 0.3%, respectively, during 24 h. The purity of the ^{4}He gas was 99.5%. Known lines from α scattering on the (gaseous) ^{4}He and solid $(Ch_2)_n$ target were used for energy calibration.

The charged reaction products were detected by means of a ΔE-E telescope placed inside the scattering chamber. The ΔE counter was a commercial Si surface barrier detector, 1000 μm thick. A side entry 31 mm thick Ge(Li) detector mounted in a separate cryostat developed in this laboratory[4,5] served as the E counter. The telescope was coupled via standard electronics to a particle identifier. The p, d, t, ^{3}He, and α-particle spectra were collected simultaneously. A Ge(Li) monitor detector was placed at a fixed angle of $\theta_{lab} = -30°$.

The telescope had two rectangular diaphragms of 9 mm thick tantalum. The rear diaphragm (2 mm $\times$ 3 mm) was placed directly in front of the ΔE detector. The front diaphragm (3 mm $\times$ 8 mm) was situated about 160 mm from the rear one. The rear diaphragm-to-target distance was about 380 mm. Two extra 9 mm thick tantalum collimators placed between the two diaphragms served to stop the unwanted high energy protons from reaching the detectors. The geometrical "G factors" for the yield to cross section conversion were calculated from the formulas given by Silverstein,[6] which were derived neglecting the diaphragm thickness and the beam diameter. Both effects could be estimated in the present case to be $\sim 1\%$ and were neglected. The beam currents were chosen in the 10–500 nA range such as to keep the dead time below 3%.

The charged particle spectra have been measured at incident energies $E_\alpha = 110$, 130, 158.5, and 172.4 MeV in the $9 \leq \theta_{lab} \leq 50°$ angular range. In the present work the theoretical analysis was concentrated mainly on the p and d spectra. The reason for it is that t, ^{3}He, and ^{4}He spectra are contaminated by contributions from the decay of the ^{5}Li, ^{5}He, and ^{4}He states, respectively, making the analysis rather ambiguous.

III. THEORETICAL TREATMENT

The experimental data have been compared with the predictions of two theoretical models.

A. The flying spectator or Serber type breakup

The model describes the breakup of the incident particle in the field of the target nucleus.[7,8] One of the constituents of the projectile is presumed to continue undisturbed, behaving like a spectator, while the remaining part interacts with the target. For the unperturbed particle the double differential cross section is expected to have the form

$$\frac{d^2\sigma}{d\Omega\, dE} \alpha\, |\psi(p)|^2 R_n(E_x) \tag{1}$$

with

$$|\vec{p}|^2 = |\vec{p}_0|^2 + 2m_x E_x - 2|\vec{p}_0|(2m_x E_x)^{1/2}\cos\theta\,,$$

where p_0, m_x, and E_x are the initial momentum of the observed particle due to the c.m. motion of the incident α particle, the mass, and the energy of the observed particle, respectively. The term labeled $R_n(E_x)$ is a term representing the final n-body phase space or density of state factor [given by the relations (4) and (5) in the next section]. To be able to calculate the corresponding phase space factors knowledge of the number of particles present in the final state is needed.

For both the p-t and d-d partitions of the α particle we have used Eckart type wave functions

$$\psi_\alpha = C\left[\frac{\gamma}{2\pi}\right]^{1/2} \frac{e^{-\gamma r}}{r}(1 - e^{-\beta r})^4\,, \tag{2}$$

where $\gamma = (2\mu\epsilon_\alpha/\hbar^2)^{1/2}$ with μ and ϵ_α being the reduced mass and the separation energy, respectively. Originally this function was employed only for the p-t representation of the α particle.[9] The value of β was taken to be 1.0 fm^{-1}. The Fourier transform of the wave function (2) is given by[10]

$$\psi_\alpha(p) = \frac{c^2}{\pi^2}(2\mu\epsilon_\alpha)^{1/2}\left\{\frac{1}{2\mu\epsilon_\alpha + p^2} - \frac{1}{[(2\mu\epsilon_\alpha)^{1/2} + \hbar\beta]^2 + p^2} + \frac{6}{[(2\mu\epsilon_\alpha)^{1/2} + 2\hbar\beta]^2 + p^2}\right.$$

$$\left. - \frac{4}{[(2\mu\epsilon_\alpha)^{1/2} + 3\hbar\beta]^2 + p^2} + \frac{1}{[(2\mu\epsilon_\alpha)^{1/2} + 4\hbar\beta]^2 + p^2}\right\} . \quad (3)$$

B. The Fermi statistical partition theory

According to a model proposed by Fermi[11] the energy in the center of mass of the colliding system is assumed to be suddenly released and distributed with equal probabilities among the various degrees of freedom in the volume of interaction. If the total angular momentum of the colliding system is taken to be equal to zero, i.e., assuming an isotropic distribution of the outgoing particles in their center of mass system, the shape of their spectrum, which is proportional to the available phase space, can be easily derived[11,12]. Delves[13] has developed a formalism to also take the other l values into account.

Though such a simplified assumption may not be justified (because of the expected non-negligible contributions from the angular momentum values different from zero), it has usually been used[14] to calculate the phase space factor for the emitted particles in the laboratory system.

For a reaction where n particles in the final channel are emitted randomly in the allowed phase space, the energy spectrum of a particular fragment at a fixed angle is governed only by the phase space distribution, as already given by many authors.[11,12] In the present work we adopt the recursion formula derived by Delbar[15] for the case of an n-particle final state:

$$\frac{d^2R_n}{dE_1 d\Omega_1}(T,P,m_1,m_2 \ldots m_n) = m_1 p_1 R_{n-1}(T,P,m_2 \ldots m_n) , \quad (4)$$

where

$$R_{n-1}(T,P,m_2,\ldots m_n) = K\left[T - \frac{P^2}{2M'}\right]^{1/2[3(n-1)-5]} . \quad (5)$$

The quantities T, M' and P are the sums of the kinetic energies and masses and the vector sum of the momenta of all particles in the final state except the detected particle, respectively. K is a constant given by the relation

$$K = \frac{2^{1/2(n-4)}\pi^{3/2(n-2)}}{\Gamma[3/2(n-2)]}\frac{(\pi_{i=2}^{n} m_i)^{1/2}}{(M')^{3/2}} . \quad (6)$$

The statistical partition model was originally developed by Fermi to explain pion production.[10] Since then the same model has been frequently used to describe the continuous background in the breakup spectra[16–18] of light nuclei.

IV. RESULTS

The proton and deuteron spectra at $E_\alpha = 172.4$ MeV are shown in Figs. 1 and 2, respectively, for all measured angles. Some representative spectra at other energies are shown in Figs. 3–5. All spectra present basically the same features; distinct peaks at the high energy end of the spectrum followed by a continuum at lower energies. In the low energy parts of the spectra taken at forward angles some additional distinctive structures are present (hatched areas in Figs. 1–5). These structures (peaks) are due to sequential pickup-breakup processes involving formation and subsequential decay of resonant (intermediate) states (see Figs. 1–5). The identification of the intermediate states involved is relatively simple and straightforward from the measured position, width, and energy shift of the peaks as function of angle. Unambiguous identification was achieved since, considering the different Q values involved and the fact that there are only four neutrons and four protons in the $\alpha + \alpha$ interaction, only a few intermediate states are possible in the energy range of interest. We conclude from the analysis that the low energy structures in the p and d spectra (hatched areas, Figs. 1–5) are due to the formation and the subsequential decay of $^5\mathrm{Li}_{\mathrm{g.s.}}$ and $^6\mathrm{Li}_{2.18}$ states, respectively. An idea of the magnitude of, e.g., the $\alpha + d \rightarrow {}^6\mathrm{Li}_{2.18} \rightarrow d + \alpha$ pickup-breakup cross section can be obtained from Fig. 2. This figure shows clearly the forward peaking of the deuteron production cross section from the pickup-breakup process as well as that from the $^4\mathrm{He}(\alpha,d)^6\mathrm{Li}_{2.18}$ stripping reaction (peak at $E_d \sim 129$ MeV in Fig. 2, $\theta_L = 10°$). Owing to the entrance

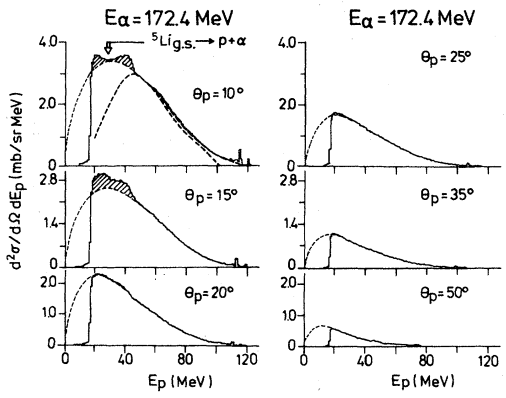

FIG. 1. Inclusive proton spectra from $\alpha + \alpha$ interactions measured at different angles at $E_\alpha = 172.4$ MeV. The thin dashed curves represent the fits obtained applying the Fermi statistical partition model. The thick dashed curve represents the prediction of the Serber mechanism for a three-body final state. The structures at low energies at 10° and 15° are due to the sequential processes as explained in the text.

channel symmetry ($\alpha + \alpha$ system), the cross section for the emission of the $^6Li_{2.18}$ recoil nucleus will also show a forward peaking. This will contribute to the above mentioned forward peaking of the deuteron production cross section from the $^6Li_{2.18} \rightarrow d + \alpha$ decay. For quantitative analysis, however, one must consider the geometry of the defining slit system of the gas target since not all of

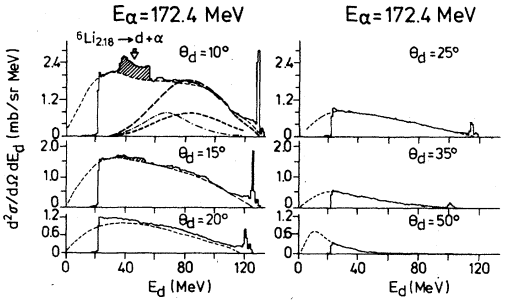

FIG. 2. Inclusive deuteron spectra from $\alpha + \alpha$ interactions measured at different angles at $E_\alpha = 172.4$ MeV. The thin dashed curves represent the fits obtained applying the Fermi statistical partition model. The thick dashed curve represents the prediction of the Serber mechanism for a three-particle final state (that curve is represented with two different normalizations); the dot-dashed curve represents the same prediction when a four-body final state is assumed. The structures at low energies at 10°, 15°, and 20° are due to the sequential processes as explained in the text.

the decay deuterons from the $^6Li_{2.18}$ emitted at a specified angle are detected by the counter telescope.

The cross section for the production of $^7Li_{4.63}$, $^6Li_{2.18}$, and ^5He or ^5Li rapidly decreases with increasing incident energy. The data for the $^7Li_{4.63}$ differential cross section at $\theta_{lab} = 10°$ are shown in Fig. 6. Such a behavior is similar to the one observed by Glagola *et al.*[19] for the formation of ^6Li, ^6He, ^7Li, and ^7Be via the same entrance channel. Although the reactions are different, this similarity in the energy behavior suggests the same kind of direct reaction mechanism for all of these processes.

As seen from Fig. 6 the cross section of the continuum parts exhibits, on the contrary, an increasing trend with energy and is by an order of magnitude larger than that for the transition to the most strongly excited levels.

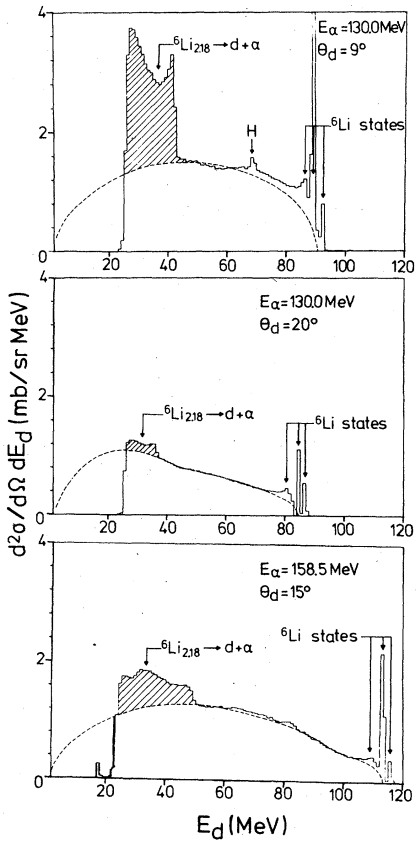

FIG. 3. Inclusive deuteron spectra from $\alpha + \alpha$ interaction measured at different energies and angles. The dashed curves are the predictions of the Fermi statistical partition model. The peak at $\sim$ 68 MeV in the 130 MeV spectrum is due to hydrogen contamination.

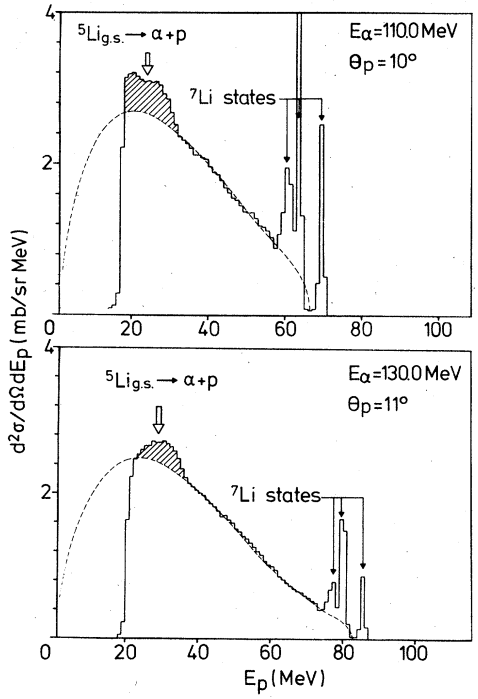

FIG. 4. Inclusive proton spectra from $\alpha + \alpha$ interactions measured at different energies and angles. The dashed curves are the predictions of the Fermi statistical partition model.

To compare the shape of the spectra with the Fermi partition model, a computer program has been written to calculate the phase space distributions for different n-body breakup processes and to perform a least squares fit to the experimental data, based on any specified combination of n-body phase spaces. At each angle the absolute and relative magnitudes of contributing n-body final state components were extracted. The theoretical curves obtained are shown together with the experimental spectra in Figs. 1—5. The distinction between different modes of breakup is subject to: (a) the shape of the phase space distributions which are distinctly different when the number of particles in the final state differs, and (b) the threshold energy of the breakup which governs the distinction between phase-space distributions of similar shapes.

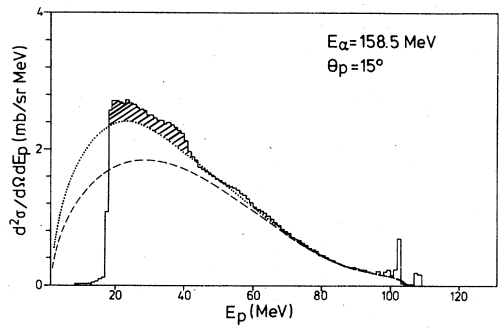

FIG. 5. Inclusive proton spectrum from $\alpha + \alpha$ interactions and its comparison with two curves predicted by the Fermi statistical partition model. The dashed curve represents the prediction of the model when only $pt\alpha$ and $pdn\alpha$ breakups are taken into account. The dotted curve is for the case when the $p - d - d - t$ breakup was added as a possibility.

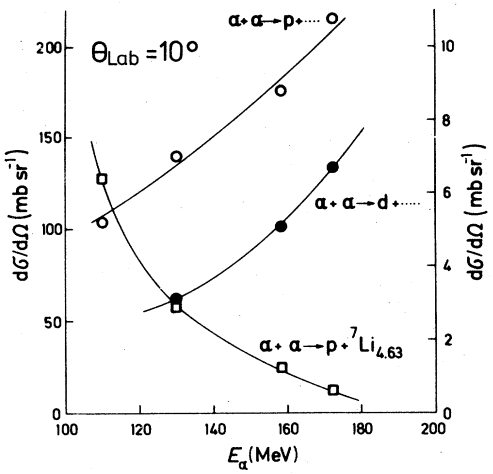

FIG. 6. Excitation function (lab) of the continuum part of the proton and deuteron spectra at $\theta_{lab} = 10°$. For comparison the excitation function (lab) for the $\alpha + \alpha \rightarrow p + {}^7Li_{4.63}$ process is shown on a different scale on the right side. The curves are to guide the eye only.

In our case a certain degree of ambiguity arises in distinguishing between complicated breakup processes with four or more particles in the final state when, e.g., both α particles are assumed to be broken (for example, the distributions for the $\alpha + \alpha \rightarrow d + d + d + d$ and $\alpha + \alpha \rightarrow d + p + t + d$ breakups are almost indistinguishable).

The differential cross sections obtained from fitting the proton and deuteron experimental spectra with the Fermi partition model are shown in Figs. 7 and 8. The breakup modes that could be unambiguously identified are labeled separately. Different combinations of breakup fragments giving almost the same quality of fit and almost the same partial contribution to the total cross section have been shown under a common label (Fig. 7, open squares).

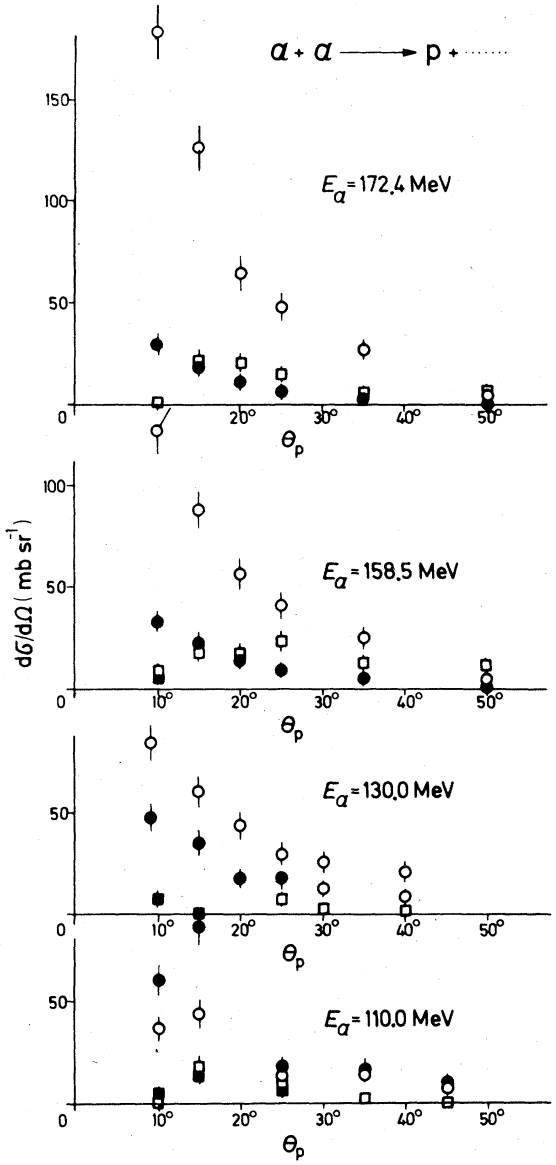

FIG. 7. Experimental angular distributions for different breakup modes at different energies extracted by the Fermi statistical partition theory to the proton inclusive spectra. The dots denote the $pt\alpha$ mode, the circles the $pdn\alpha$, the solid squares the $pn\,^6Li_{2.18}$ mode, and the open squares the more complicated breakup modes (see text).

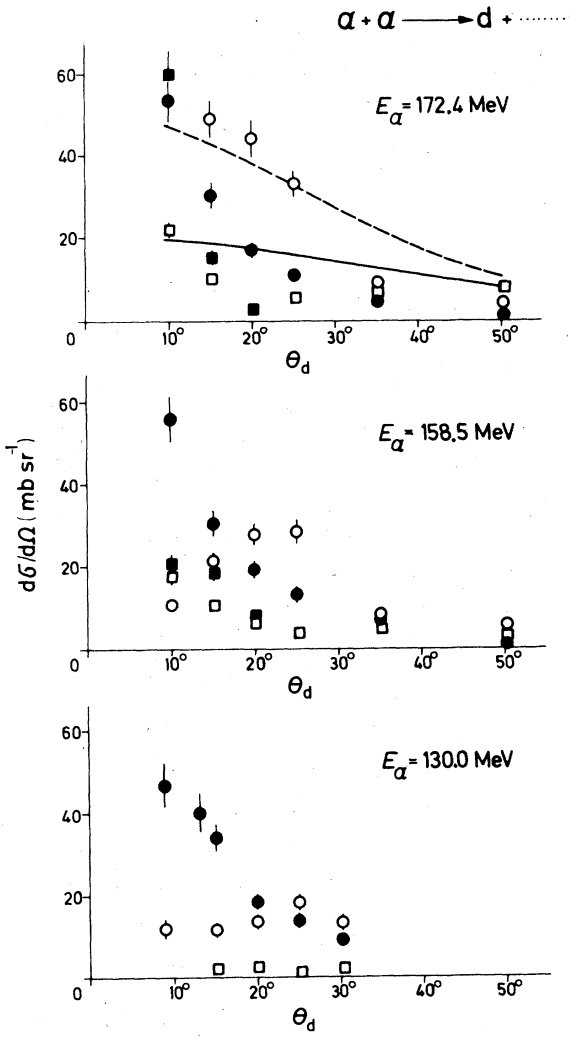

FIG. 8. Same as Fig. 7 but for the deuteron spectra. The dots denote the $dd\alpha$ mode, the circles the $dpn\alpha$ mode, the solid squares the $dt\,^3He$ mode, and the open squares the more complicated breakups (see text). The full and dashed lines show the expected distribution from the Fermi statistical partition model for the $dd\alpha$ and $dpn\alpha$ breakup modes, respectively.

To test for the possible contribution of a quasifree breakup to the continuum, some theoretical spectra have been calculated in the framework of the Serber mechanism. The spectra are shown for $\theta = 10°$ at $E_\alpha = 172.4$ MeV (Figs. 1 and 2) where the contribution of such a mechanism is expected to be the largest.[20]

In the case of the deuteron spectrum, the theoretical energy distributions were calculated assuming both three and four particles in the final state, since the number of particles in the final state influences the phase factor in Eq. (1). The curves obtained are shown in Figs. 1 and 2.

V. DISCUSSION AND CONCLUSIONS

The analysis of the breakup spectra of protons and deuterons has shown that a large part of the

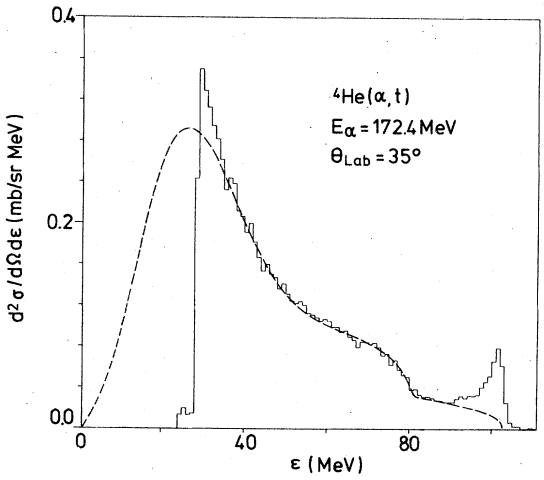

FIG. 9. Inclusive triton spectrum at $\theta_{lab} = 35°$, $E_\alpha = 172.4$ MeV. The dashed curve is the fit obtained with the Fermi model.

breakup cross section can be attributed to the statistical partition of the intermediate system.

From the comparison of the continuum part of the proton and deuteron experimental spectra with the predictions of the applied model it is seen that the Fermi statistical partition model gives very satisfactory agreement to the overall shape of the spectra. However, at forward angles the p and d spectra exhibit an enhancement above the theoretical prediction of the Fermi partition model at $50 \leq E_p \leq 80$ MeV and at $60 \leq E_d \leq 80$ MeV, respectively. As shown by the theoretical curves calculated using the Serber mechanism one cannot rule out a small contribution from this mechanism.

The experimental angular distributions for different breakup modes are given in Figs. 7 and 8. The differential cross sections indicate that, according to the Fermi partition model, the process is not purely isotropic in the center of mass system. The theoretical cross sections calculated from the Fermi partition model (assuming isotropy) in the c.m. system) are shown for two modes of decay in Fig. 8. It is seen that the fits of the model for the angular distributions are much less satisfactory than in the case of the spectral shapes. The agreement in the shape of the spectra can be understood under the assumption that anisotropy in the center of mass does not affect the spectral shape too much. It is also necessary to say that isotropy is not a requirement of Fermi's model, as it was pointed out by Hagedorn.[21] The isotropy was introduced only to make the calculations possible at this stage.

The mode of decay and multiplicity of particles in the final state are a function of the incident energy. This is illustrated in Figs. 7 and 8. Also noteworthy is the fact that the overall contribution of the breakup into the continuum increases considerably with energy.

In the case of the deuteron spectra one observes a rapid change of the dominant modes of breakup; namely at 158.5 and 172.4 MeV, the $d - t - {}^3$He breakup should be included to obtain a satisfactory fit to the experimental data, while at 130 MeV this mode is apparently very weak and not observed. It is interesting that this mode of breakup is very difficult to explain as a direct reaction. The fusion of the two alphas and subsequent fragmentation seem to be much more probable as an explanation. To demonstrate that the presence of the $d - t - {}^3$He breakup mode is real, we show a triton spectrum taken at 172.5 MeV and $\theta_{lab} = 35°$. In Fig. 9 the fit to the data is made with the Fermi statistical partition model and it clearly shows the onset of the $d - t - {}^3$He breakup at $E_t = 81$ MeV.

The pattern of remarkably good fits to the continuum, using combinations of phase space distribution has been also observed in other reactions, e.g., ${}^9\text{Be}(p,\alpha)X$.[15]

The agreement between the data and the Fermi statistical partition model indicates that: (i) the emitted particles forming the continuous spectra mainly stem from processes involving very low partial waves, and furthermore, (ii) the colliding system at these low partial waves appears to form a fused system allowing total energy sharing among all participating particles, followed by an explosion in the available phase space.

For reactions among light nuclei, this mechanism which has already been extensively used in high energy physics,[21] therefore constitutes an important supplement to the peripheral phenomena involved in two-body or quasi-two-body processes,[22–25] which usually include only higher partial waves of the relative motion of the particles in the incident channel.

ACKNOWLEDGMENTS

The authors gratefully acknowledge the participation of Dr. C. Alderliesten in the first stages of this work. The help of Dr. Riepe and Mr. Protić in producing high quality germanium detectors has been instrumental in achieving this experiment. The help of Dr. R. Shyam in the computation of the

Serber model is gratefully acknowledged. The discussions with Th. Delbar and Dr. Gh. Gregoire have been useful in broadening our understanding and are gratefully acknowledged.

[1]W. von Witsch, G. S. Mutchler, and D. Miljanić, Nucl. Phys. A248, 485 (1975).
[2]I. Šaus, *Proceedings of the International Conference on Nuclear Structure, Tokyo, 1977,* edited by T. Marumori (Physical Society of Japan, Tokyo, 1978), p. 57 and references therein.
[3]I. M. Duck and V. Valković, Lett. Nuovo Cimento 8, 537 (1973).
[4]G. Riepe and D. Protić, Nucl. Instrum. 101, 77 (1972).
[5]G. Riepe and D. Protić, IEEE Trans. Nucl. Sci. 22, 178 (1975).
[6]E. Silverstein, Nucl. Instrum. 101, 77 (1972).
[7]R. Serber, Phys. Rev. 72, 1008 (1947).
[8]J. R. Wu, C. C. Chang, and H. D. Holmgren, Phys. Rev. Lett. 40, 1013 (1978).
[9]T. K. Lim, Phys. Lett. 44B, 341 (1973).
[10]R. Shyam (private communication).
[11]E. Fermi, Prog. Theor. Phys. 5, 570 (1950).
[12]A. M. Baldin, V. I. Goldanskii, and I. L. Rozenthal, *Kinematics of Nuclear Reactions* (Pergamon, New York, 1961), p. 87.
[13]L. M. Delves, Nucl. Phys. 20, 275 (1960).
[14]S. Tanaka *et al.*, Nucl. Phys. A341, 199 (1980).
[15]T. Delbar (private communication).
[16]M. P. Barker, J. M. Cameron, N. S. Chant, and N. F. Mangelson, Nucl. Phys. A184, 97 (1972).
[17]R. B. Weisenmiller, N. A. Jelley, D. Ashery, K. H. Wilcox, G. J. Wozniak, M. S. Zisman, and J. Cerny, Nucl. Phys. A280, 217 (1977).
[18]J. A. Koepke and R. E. Brown, Phys. Rev. C 16, 18 (1977).
[19]B. G. Glagola, G. J. Mathews, H. F. Breuer, V. E. Viola, Jr., P. G. Roos, A. Nadasen, and Sam A. Austin, Phys. Lett. 41, 1698 (1978).
[20]J. R. Wu, C. C. Chang, H. D. Holmgren, and R. W. Koontz, Phys. Rev. C 20, 1284 (1979).
[21]R. Hagedorn, Nuovo Cimento 15, 434 (1960).
[22]T. Sawada, G. Paić, M. B. Epstein, and J. G. Rogers, Nucl. Phys. A141, 169 (1970).
[23]G. Paić, J. C. Young, and D. J. Margaziotis, Phys. Lett. 32B, 437 (1970).
[24]C. Alderliesten, A. Djaloeis, J. Bojowald, C. Mayer-Böricke, G. Paić, and T. Sawada, Phys. Rev. C 18, 2001 (1978).
[25]A. Djaloeis, J. Bojowald, C. Alderliesten, C. Mayer-Böricke, G. Paić, and Ž. Bajzer, Nucl. Phys. A273, 29 (1976).